M. J. CONDENSED MATTER VOLUME 5, NUMBER 1 1 JANUARY 2004

Phase Diagram of Ferrimagnetic System with Triangular Symmetry: Spin and Anisotropy Effects

M. Aouzi and M. El Hafidi
Laboratoire de Magnétisme & de Physique des Matériaux, Faculté des Sciences Ben M'sik, Département de Physique, B.P 7955, Casablanca 20453, Morocco

The magnetic properties (phase diagram and magnetization) of a ferrimagnetic system, consisting of two magnetic sublattices (A and B) with different spins (S_A=$\frac{1}{2}$ and $S_B\rangle\frac{1}{2}$) and different interactions coupling together, are investigated within the framework of the effective -field theory with correlations. Furthermore, each considered sublattice has in-plane triangular symmetry requiring a coordination number of magnetic atoms $z = 6$ which may affect the general magnetic behavior of the system. The effects of crystal-field interaction D_B in the sublattice B (with $S_B\rangle\ \frac{1}{2}$) on the magnetic properties are examined in detail. Because of the higher coordination number and different kinds of interactions acting on the system of spins, we find a number of interesting phenomena: (i) the temperature dependence of the total magnetization shows many characteristic behaviors depending on D_B and S_B, (ii) the presence of compensation points is conditioned by the given values of different parameters while the second order transition temperatures are studied according to each specific circumstance. The aspects of interest in this study is mainly the higher coordination number of magnetic species and the realistic interactions which are taken into account. This model can be relevant for understanding the magnetic behaviors of the new class of lamellar oxides AMO_2 (A = Li, Na, Na,..; M = Ni, Fe, Co,..).

PACS numbers: 75.10.-b ; 75.10.Jm ; 75.10.Jm ;75.50.Gg ;

I. INTRODUCTION

Ferrimagnetic systems constitute a special class of materials which have regained interest because of their richness from the theoretical point of view and their usefulness in advanced modern technologies such high speed digital recording.

Theoretically, great emphasis has been given to the examination of the spin arrangement as well as the kinds of couplings governing the magnetic behavior of the two-sublattice Ising models. Different techniques have been used such mean-field approximation (MFA) [1], [2], [3],effective-field theory with correlations (EFT) [4], [5], Bethe-Peierls method (BPM) [6], renormalization-group approach (RGA) [7], [8], high-temperature series expansions (HTSE) [9] and Monte Carlo simulation (MCS) [10]. However, few studies have been devoted to the Ising spin ferrimagnetic systems with crystal-field interaction and a coordination number upper than 4 in presence of intra- and inter-sublattices exchange interactions except a partial treatment within the works of Tucker [11] and Fresneau et al. [12]. In fact, the problems are difficult to resolve either analytically or computationally and there is a need for complementary experimental works to focus the theoretical efforts.

The main purpose of this work is thus to study the magnetic properties of a two-sublattice ferrimagnetic Ising system consisting of two kinds of magnetic atoms A and B with spins S_A ($S_A = \frac{1}{2}$) and S_B ($S_B > \frac{1}{2}$) located in triangular site symmetry. Besides the exchange couplings between spins, the uniaxial crystal-field interaction D_B acting on the B atoms is also taken into account. We discuss, within the effective-field theory with correlations (EFT) [13], [14], the effects of S_B and D_B parameters on the magnetic properties of the system (compensation and critical temperatures, sublattice's and global magnetizations). Our original contribution concerns especially the triangular in-plane lattice symmetry which leads to a higher coordination number ($z = 6$) that should affect seriously the magnetic behavior of the system. This situation may be found in the case of lamellar oxides such $AM_xM'_{1-x}O_2$ where A = Li^+, Na^+; M,M' = Ni^{l+}, Co^{l+}, Fe^{l+},...., and $l = 2$ or 3. In these compounds, each $3d$ ion occupies the center of an octahedral site and the whole of these sites forms a triangular lattice. Thus, the compound can be regarded as a package of alternative triangular layers $..A - B - A - B..$, in the third direction ($\overrightarrow{c}$ axis) as depicted shematically in figure1 [15]; [16]; [17].

This class of materials has known in the last decennia a peculiar essor especially in the energy storage and long life batteries fabrication. They are also important since they may be prototypes on which certain concepts such the magnetic frustrations or spin glasses can be tested [15], [18].

Graphite Bi-intercalation compounds (GBIC's) offer another opportunity for the application of this model. In these materials, the inter-layer graphite space can easily receive a great variety of intercalant species. Layered transition-metal chlorides, namely $CoCl_2$, $NiCl_2$, $MnCl_2$, $FeCl_3$ and $CrCl_3$ have proved to be very useful as magnetic intercalants [19] ; [20] ; [21], [22]. In the pristine transition-metal chloride, the 3d ions lattice has a hexagonal or triangular layered crystal structure (for respectively trivalent and divalent metal) and it remains almost unchanged after intercalation. With two intercalants MCl_n and $M'Cl_{n\prime}$, the sequence along the $\overrightarrow{c}$ direction becomes ..G-MCl_n-G-$M'Cl_{n'}$-G..., where G designs the graphite layer separating the two intercalants.

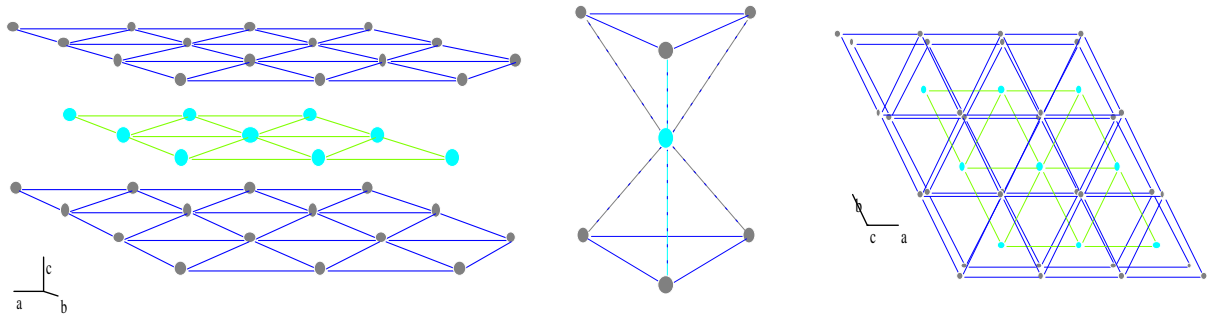

FIG. 1: The placement of the magnetic ions A with spin $S_A = \frac{1}{2}$ (black circles) and B with spin $S_B > \frac{1}{2}$ (white circles) in the repeating structure of layers along the $\vec{c}$–axis (a) and the interlayer coordination illustration of a selected ion B (b). The exchange interactions J_{AA} , J_{AB} and J_{BB} are also indicated.

The theoretical framework used here (EFT) is superior to the standard mean-field theory (MFT) and has been successfully applied to a variety of Ising problems. This approach takes into account for the generalized spins, the correlations effects known to be important especially near the critical temperatures. A review of certain principles of this approach has been given by Kaneyoshi [14],[23].

In this work, therefore, the spin S_A of the sublattice A is fixed at $S_A = \frac{1}{2}$ and the spin S_B of the sublattice B is taken at an arbitrary value ($S_B = 1$ or $\frac{3}{2}$).

Since $S_B > \frac{1}{2}$, the crystal-field term is then included in the sublattice B and the effects of D_B on the magnetic properties of the layered system are examined in detail especially for $D_B \leq 0$.

The outline of this paper is as follows. The formulation of the problem is given in section II on the basis of the exact Ising spin identities [24] ; [25] as well as the differential operator technique [14]. The exact formulation of the total magnetization in the system is derived and compared with the previous results derived for $D = \infty$ and for $z \leq 4$ [27]. It is shown that if a compensation temperature exists in the system, its behavior as a function of D_B may be dramatically modified by changing the spin S_B from the integer value ($S_B = 1$) to the half-integer value ($S_B = \frac{3}{2}$) .

Then, the EFT is applied to the calculation of the sublattices and the global magnetizations . In section III, the two-sublattice system is investigated within the EFT, selecting the two values of S_B, namely $S_B = 1$ and $S_B = \frac{3}{2}$.

In this section, a number of interesting phenomena, concerning compensation points, transition temperatures and the magnetization behavior are pointed out. A calculation of compensation, critical temperatures and magnetization is also presented explicitly for given values of spin S_B. In section IV, we discuss and comment on the obtained results.

II. FORMULATION

We consider a ferrimagnetic Ising spin system. The underlying lattice is divided into two sublattices A and B where each sublattice has the same triangular structural symmetry requiring a coordinate number $z = 6$. A site of the sublattice A is occupied by spin-1/2 ($S_A = \frac{1}{2}$), while the spin on the B site is allowed to take an arbitrary value ($S_B = 1$ or $\frac{3}{2}$).

The exchange interaction between A and B magnetic species is assumed to be antiferromagnetic.

Furthermore, we assume that there exist a ferromagnetic exchange interactions between every nearest-neighbor pair of A or B atoms. For clarification, the assumed exchange couplings in the system are indicated in figure 1.

Thus, in absence of external magnetic field, the Hamiltonian of the system takes the form:

$$H = J_{AB} \sum_{im} S_{iA}^z S_{mB}^z - J_{AA} \sum_{ij} S_{iA}^z S_{jA}^z - J_{BB} \sum_{mn} S_{mB}^z S_{nB}^z - D_B \sum_{m} (S_{mB}^z)^2 \qquad (1)$$

where the first three summations are taken over all the nearest-neighbor pairs in the lattice, whereas $S_{iA}^z = \pm\frac{1}{2}$ is the usual z-component of spin moment on the A atom, and S_{mB}^z is the spin operator on the B atom. D_B is the crystal-field interaction acting on the spin S_B.

There exist three coupling constants ($J_{AA} \geq 0$, $J_{BB} \geq 0$ and J_{AB}) depending on where the spin pair is located.

For an arbitrary chosen atom α ($\alpha = A$ or B), the magnetization per site is given by:

$$m_\alpha = \left\langle S^z_{i,\alpha} \right\rangle \tag{2}$$

where the brackets mean the statistical average.

The problem is for instance the evaluation of the mean values $\langle S^z_{iA}\rangle$ and $\langle S^z_{mB}\rangle$. we start with exact Ising spin identities given established by [24] and [26].

Using the differential operator technique introduced initially in these identities by Honmura and Kaneyoshi [13], the mean values $\langle S^z_{iA}\rangle$ and $\langle S^z_{mB}\rangle$ are then given by:

$$m_A = \left\langle \left\{ \prod_{\delta=1}^{z} \exp(-J_{AB}\nabla S^z_{i+\delta B}) \right\} \left\{ \prod_{\delta'=1}^{z'} \exp(J_{AA}\nabla S^z_{i+\delta' A}) \right\} \right\rangle f_A(x) \mid_{x=0} \tag{3}$$

and

$$m_B = \left\langle \left\{ \prod_{\delta=1}^{z} \exp(J_{BB}\nabla S^z_{i+\delta B}) \right\} \left\{ \prod_{\delta'=1}^{z'} \exp(-J_{AB}\nabla S^z_{i+\delta' A}) \right\} \right\rangle f_B(x) \mid_{x=0} \tag{4}$$

where $\nabla = \frac{\partial}{\partial x}$ is a differential operator, δ and δ' denote the nearest-neighbors of the central site i or m respectively, and $z_i (z = z' = 6)$ is the coordination number.

The function $f_A(x)$ in 3(5) is defined by

$$f_A(x) = \frac{1}{2}\ tanh(\frac{1}{2}\beta\ x) \tag{5}$$

where $\beta = \frac{1}{k_B T}$

and the function $f_B(x)$ which depends on the spin value S_B , is given by

$$f_B(x) = \frac{2\sinh(\beta x)}{2cosh(\beta x) + \exp(-\beta D_B)} \tag{6}$$

for $S_B = 1$ and

$$f_B(x) = \frac{1}{2}\ \frac{3\sinh(\frac{3\beta x}{2}) + \exp(-2\beta D_B)\sinh(\frac{\beta x}{2})}{cosh(\frac{3\beta x}{2}) + \exp(-2\beta D_B)\cosh(\frac{\beta x}{2})} \tag{7}$$

for $S_B = \frac{3}{2}$

Furthermore, with the help of the van der Waerden identity for spin operators $S^z_{iA} = \pm\frac{1}{2}$,

$$exp(aS^z_{iA}) = \cosh(\frac{a}{2}) + 2S^z_{iA}\sinh(\frac{a}{2}) \tag{8}$$

the exact identity (3) and (4) can be written as:

$$m_A = \left\langle \prod_{\delta=1}^{z} [\cosh(\frac{J_{AA}}{2}) + 2S^z_{iA}\sinh(\frac{J_{AA}}{2})]\ \prod_{\delta'=1}^{z'} \exp(-J_{AB}\nabla S^z_{i+\delta B}) \right\rangle f_A(x) \mid_{x=0} \tag{9}$$

and

$$m_B = \left\langle \prod_{\delta=1}^{z} [\cosh(\frac{J_{AB}}{2}) - 2S^z_{iA}\sinh(\frac{J_{AB}}{2})]\ \prod_{\delta'=1}^{z'} \exp(J_{BB}\nabla S^z_{i+\delta B}) \right\rangle f_B(x) \mid_{x=0} \tag{10}$$

Now, in order to treat the identities (9) and (10) further, we need the van der Waerden identity for S^z_{mB}.

Generally, we can use the van der Waerden identity for an arbitrary S [14], [13]

$$exp(-bS^z) = \sum_{n=0}^{2S} A_n(b)(-S^z)^n \tag{11}$$

which gives

$$\exp(-bS^z_{i+\delta B}) = 1 - \ S^z_{i+\delta B}\sinh(b) + (S^z_{i+\delta B})^2[\cosh(b) - 1] \tag{12}$$

for $S_B = 1$ and

$$exp(-bS^z_{i+\delta B}) = A(b) - \ B(b)S^z_{i+\delta B} + C(b)(S^z_{i+\delta B})^2 - D(b)(S^z_{i+\delta B})^3 \tag{13}$$

for $S_B = \frac{3}{2}$ where

$$A(b) = \frac{1}{8}[9cosh(\frac{b}{2}) - cosh(\frac{3b}{2})] \tag{14}$$

$$B(b) = \frac{1}{27}[27sinh(\frac{b}{2}) - sinh(\frac{3b}{2})] \tag{15}$$

$$C(b) = \frac{1}{2}[cosh(\frac{3b}{2}) - cosh(\frac{b}{2})] \tag{16}$$

$$D(b) = \frac{1}{3}[sinh(\frac{3b}{2}) - 3sinh(\frac{b}{2})] \tag{17}$$

Even if we use the van der Waerden identity (11), it is generally impossible to calculate the sublattices magnetizations m_A and m_B exactly, although the system with $D = \infty$ studied in [14] is the exceptional case. Here, as a simple procedure to use these identities for the evaluation of m_A and m_B, we introduce the approximation

$$\left\langle \prod_{\delta=1}^{z'} exp(-bS^z_{i+\delta B}) \right\rangle \sim \prod_{\delta=1}^{z'} \left\langle exp(-bS^z_{i+\delta B}) \right\rangle = \prod_{\delta=1}^{z'} \sum_{n=0}^{2S} A_n(b) \left\langle (-\ S^z_{i+\delta B})^n \right\rangle \tag{18}$$

The approximation which is of Zernike decoupling type, has been called the effective-field theory with correlations (EFT) [13], [26]. Within the EFT, the sublattices magnetizations m_A and m_B are now given respectively by:

$$m_A = [1 - m_B sinh(J_{AB}\nabla) + q(cosh(J_{AB}\nabla) - 1)]^{z'}.[cosh(\frac{J_{AA}}{2}\nabla) + 2m_A sinh(\frac{J_{AA}}{2}\nabla)]^z f_A(x) \mid_{x=0} \tag{19}$$

$$m_B = [1 + m_B sinh(J_{BB}\nabla) + q(cosh(J_{BB}\nabla) - 1)]^{z'}.[cosh(\frac{J_{AB}}{2}\nabla) - 2m_A sinh(\frac{J_{AB}}{2}\nabla)]^z f_B(x) \mid_{x=0} \tag{20}$$

for $S_B = 1$,

$$m_A = [\cosh(\frac{J_{AA}}{2}) + 2m_A \sinh(\frac{J_{AA}}{2})]^z.[A(J_{AB}) - \ m_B B(J_{AB}) + qC(J_{AB}) - rD(J_{AB})]^{z'} f_A(x) \mid_{x=0} \tag{21}$$

and

$$m_B = [\cosh(\frac{J_{AB}}{2}\nabla) - 2m_A \sinh(\frac{J_{AB}}{2}\nabla)]^{\ z}. \times [A(J_{BB}\nabla) + m_B B(J_{BB}\nabla) + qC(J_{BB}\nabla) + rD(J_{BB}\nabla)]^{z'} f_B(x) \mid_{x=0} \tag{22}$$

for $S_B = \frac{3}{2}$
where the parameters q and r are defined by:

$$q = \left\langle (S^z_{i+\delta B})^2 \right\rangle = [1 + m_B sinh(J_{BB}\nabla) + q(cosh(J_{BB}\nabla) - 1)]^{z'}.[cosh(\frac{J_{AB}\nabla}{2}) - 2m_A sinh(\frac{J_{AB}\nabla}{2})]^z f_C(x) \mid_{x=0} \quad (23)$$

and

$$r = \left\langle (S^z_{i+\delta B})^3 \right\rangle = [1 + m_B sinh(J_{BB}\nabla) + q(cosh(J_{BB}\nabla) - 1)]^{z'}.[cosh(\frac{J_{AB}\nabla}{2}) - 2m_A sinh(\frac{J_{AB}\nabla}{2})]^z f_D(x) \mid_{x=0} \quad (24)$$

for $S_B = 1$,

where the functions $f_C(x)$ and $f_D(x)$ depend on the value of S_B. They are given by:

$$f_C(x) = \frac{2\cosh(\beta x)}{2cosh(\beta x) + \exp(-\beta D)} \quad (25)$$

for $S_B = 1$ and

$$f_C(x) = \frac{1}{4}.\frac{9\cosh(\frac{3\beta x}{2}) + \exp(-2\beta D)\cosh(\frac{\beta x}{2})}{cosh(\frac{3\beta x}{2}) + \exp(-2\beta D)\cosh(\frac{\beta x}{2})} \quad (26)$$

for $S_B = \frac{3}{2}$

$$f_D(x) = \frac{1}{8}.\frac{27\sinh(\frac{3\beta x}{2}) + \exp(-2\beta D)\sinh(\frac{\beta x}{2})}{cosh(\frac{3\beta x}{2}) + \exp(-2\beta D)\cosh(\frac{\beta x}{2})} \quad (27)$$

for $S_B = \frac{3}{2}$

III. MAGNETIC PROPERTIES OF FERRIMAGNETIC SYSTEM WITH $S_B = 1$ AND $S_B = \frac{3}{2}$: APPLICATION TO THE TRIANGULAR LATTICE ($z = 6$)

In this section, let us study the phase diagrams and thermal dependences of magnetizations for the two-sublattice system with triangular symmetry ($z = 6$).

A. Sublattice magnetizations m_A with $S_B = 1$:

Substituting $z = z' = 6$ into Eq. (19) and expanding the right-hand side of (19) operating the differential operator, we can easily get the following coupled equation:

$$\begin{aligned} m_A &= K_1(m_B) + 12m_A K_2(m_B) + 60m_A^2 K_3(m_B) + \\ &\quad 160m_A^3 K_4(m_B) + 240m_A^4 K_5(m_B) + 190m_A^5 K_6(m_B) + 64m_A^6 K_7(m_B) \end{aligned} \quad (28)$$

where

$$K_i(m_B) = L_{i1} - 6m_B L_{i2} + 15m_B^2 L_{i3} - 20m_B^3 L_{i4} + 15m_B^4 L_{i5} - 6m_B^5 L_{i6} + m_B^6 L_{i7}$$

where the coefficients L_{ij} $(i, j = 1 - 7)$ can be easily derived from (19), such as:

$$L_{11} = [1 - m_B \sinh(J_{AB}\nabla) + q[\cosh(J_{AB}\nabla) - 1]^6.cosh^6(\frac{J_{AA}\nabla}{2}) f_A(x) \mid_{x=0}$$

and so on.

B. Sublattice magnetization m_B with $S_B = 1$:

Substituting $z = z' = 6$ into Eq. (20), and expanding the right-hand side of (20) operating the differential operator, we obtain easily the following coupled equation:

$$\begin{aligned} m_B &= P_1(m_B) - 12m_A P_2(m_B) + 60m_A^2 P_3(m_B) - \\ &\quad 160m_A^3 P_4(m_B) + 240m_A^4 P_5(m_B) - \\ &\quad 190m_A^5 P_6(m_B) + 64m_A^6 P_7(m_B) \end{aligned} \quad (29)$$

where

$$P_i(m_B) = T_{i1} + 6m_B T_{i2} + 15m_B^2 T_{i3} + 20m_B^3 T_{i4} + 15m_B^4 T_{i5} + 6m_B^5 T_{i6} + m_B^6 T_{i7}$$

where the coefficients T_{ij} $(i, j = 1 - 7)$ can be easily

derived from (20), such as:
$T_{11} = [1 + m_B \sinh(J_{BB}\nabla) + q[\cosh(J_{BB}\nabla) - 1]^6 . cosh^6(\frac{J_{AB}\nabla}{2}) f_B(x) \mid_{x=0}$

C. Biquadratic moment q with $S_B = 1$

Substituting $z = z' = 6$ into (23), and expanding the right-hand side of (23) operating the differential operator, we can easily get the following coupled equation:

$$q = N_1(m_B) - 12m_A N_2(m_B) + 60m_A^2 N_3(m_B) - 160m_A^3 N_4(m_B) + 240m_A^4 N_5(m_B) - 190m_A^5 N_6(m_B) + 64m_A^6 N_7(m_B)$$

with

$$N_i(m_B) = B_{i1} + 6m_B B_{i2} + 15m_B^2 B_{i3} + 20m_B^3 B_{i4} + 15m_B^4 B_{i5} + 6m_B^5 B_{i6} + m_B^6 B_{i7}$$

where the coefficients B_{ij} $(i, j = 1 - 7)$ can be easily derived from (23), such as:

$$B_{11} = [1 + m_B \sinh(J_{BB}\nabla) + q[\cosh(J_{BB}\nabla) - 1]^6 . cosh^6(\frac{J_{AB}\nabla}{2}) f_C(x) \mid_{x=0}$$

A similar procedure may be applied in the case of $S_B = \frac{3}{2}$. The set of the coupled equations (28)-(30) constitute the basis of the present work.

D. Calculations procedure

1. *Transition temperature with $S_A = \frac{1}{2}$ and $S_B = 1$ or $S_B = \frac{3}{2}$*

In order to determine the transition temperature T_C, it is necessary to solve the coupled Eqs.(28)-(30) numerically. The usual argument that the sublattices magnetizations tend to zero as the temperature approaches a critical temperature allows us to consider only linear terms in each sublattice magnetization for Eqs. (28) and (29). Consequently, all terms of the order higher than linear in (28) and (29) can be neglected. From this procedure, we obtain the following matrix equation.

$$[A] \begin{pmatrix} m_A \\ m_B \end{pmatrix} = 0 \tag{30}$$

Then, the second-order phase- transition temperature T_C can be determined from

$$det[A] = 0 \tag{31}$$

where the parameter q can be determined at $T = T_C$ from:

$$q = B_{11} \tag{32}$$

¿From the formal solutions of Eq. (32), we choose those corresponding to the highest possible transition temperature which really separates the paramagnetic phase from the other ordering phases.

To elucidate the nature of the eventual transition, let us recall that in the bulk spin-one Ising model with a crystal-field constant D, it is well known that there exists a tricritical point in the phase diagram at which the transition changes from second order to first order , the tricritical behavior is found at a negative value of D [4]. In such a system, the tricritical point can be determined from the magnetization as a special point. As discussed in the litterature[4], the bulk magnetization m_b can be written, in the vicinity of second-order transition line as:

$$m_b^2 = \frac{1 - a}{b} \tag{33}$$

whre the second-order transition line can be determined by solving $a = 1$ under the condition of $b\langle 0$. If $b\rangle 0$, the right hande side becomes negative while the left hand side of (34) is positive. If this happeans, the transition is of the first order and hence, the point at which $a = 1$ and $b = 0$ is the tricritical point.

Now, the extension of the bulk argument to the present problem with $S_B = 1$ is not so easy, since we have two order parameters (m_A and m_B) which are coupled complexly.

So, let us assume that even in the region near tricritical point the magnetization m_A can be given by, upon taking only the linear terms of m_A in Eq. 28,

$$m_A = \frac{U_2 m_B}{1 - U_1 - U_3 m_B^2} \tag{34}$$

By using (34), we can rewrite the magnetization m_A in the from:

$$m_A^2 = \frac{1-\overline{a}}{\overline{b}} \tag{35}$$

where the expressions of $\overline{a}$ and $\overline{b}$ given in appendix A.

Here, the condition ($\overline{a} = 1$) is equivalent to evaluating the relation (32). The right-hand side of (36) must be positive. If it is not the case, the transition is of the first order, and hence the point at which $\overline{a} = 1$,$\overline{b} = 0$ is the tricritical point.

IV. COMPENSATION TEMPERATURE WITH $S_A = \frac{1}{2}$ AND $S_B = 1$ OR $S_B = \frac{3}{2}$

As known, in a ferrimagnet, the sublattice magnetizations don't have the same sign, and there may be a compensation temperature $T_{Comp} \leq T_C$ at which the total magnetization reduces to zero, even though $m_A \neq 0$ and $m_B \neq 0$. Thus, the compensation temperature can be determined by introducing the condition $m_A = -m_B$ into the coupled Eqs.(28) - (30).

V. NUMERICAL RESULTS AND DISCUSSION

In this section, we present and examine the numerical results concerning the phase diagrams and the temperature dependences of magnetization in the two-sublattice system in two spin cases ($S_A = \frac{1}{2}$; $S_B = 1$) and ($S_A = \frac{1}{2}$; $S_B = \frac{3}{2}$) for some selected values (J_{AB},J_B,D).

A. Phase diagram of the system $S_A = \frac{1}{2}$ and $S_B = 1$

In Fig.2.a, we have shown the phase diagram of the two-sublattice system with $S_A = \frac{1}{2}$ and $S_B = 1$ in the $(T/J_A, D/J_A)$ plane. The value of J_B/J_A is fixed at 0.25 and the value of J_{AB}/J_A is changed , $J_{AB}/J_A = 0.05$ (curve a); $J_{AB}/J_A = 0.1$ (curve b) ; $J_{AB}/J_A = 0.25$ (curve c), $J_{AB}/J_A = 0.5$ (curve d) and $J_{AB}/J_A = 1.0$ (curve e). In this figure, the solid lines denote the second-order transition ($\overline{a}$=1, $\overline{b}_1\langle 0$).The dashed line parts express the first-order phase transition, while the thick line describes the tricritical points determined from the condition ($\overline{a} = 1$, $\overline{b}_1 = 0$). It is seen that the critical temperature changes continuously when D moves from the positive to negative values. Qualitatively, the same behavior is observed for different value of the J_B/J_A ratio, although for small values (positive or negative) of D, the effect of the inter-layer coupling is quite visible and T_C increases considerably with J_B/J_A. Indeed, for a large negative value of D, the only ground states of spin $\frac{1}{2}$ and spin 1 are respectively $\pm\frac{1}{2}$ and 0, since these values of D are favorable for an in-plane confinement of the S_B spins. In this limits, T_C takes its value essentially from the A ions contribution. In the same figure, the black points denote the particular negative values of the D at which the ground state of the sublattice B must be the $S_B^z = 0$ state. Whereas, for positive values of D , the Ising character is enhanced and when $D \to +\infty$, the spin operators S_B can attain their highest eigenvalues ($|S_B^z|$ = 1) which correspond to the ground state configuration of the Hamiltonian (1).

In figure 2.b, we have reported for a fixed value of J_B/J_A at 0.25 and for each selected value of J_{AB}/J_A , the corresponding compensation temperature (dashed curves). The termination of these curves (at their upper end) occurs when T_{comp} is equal to the transition temperature T_C. Notice that T_{comp} exists only in a relatively narrow interval of single-ionic anisotropy D and relatively low of the ratio J_{AB}/J_A:, $J_{AB}/J_A = 0.05$(curve a); $J_{AB}/J_A = 0.1$(curve b) ; $J_{AB}/J_A = 0.25$(curve c). Some similar results concerning T_c and T_{comp} have been obtained by in the case of bilayer ferrimagnetic square system with a coordination number $z = 4$ [28].

B. Phase diagram of the system $S_A = \frac{1}{2}$ and $S_B = \frac{3}{2}$

In Fig 3, we have shown the phase diagram of the two-sublattice system with $S_A = \frac{1}{2}$ and $S_B = \frac{3}{2}$ when the value of D/J_A is changed. The value of J_B/J_A is fixed at 0.01 and the value of J_{AB}/J_A is changed, $J_{AB}/J_A = 0.05$ (curve a); $J_{AB}/J_A = 0.1$ (curve b); $J_{AB}/J_A = 0.15$ (curve c) ; $J_{AB}/J_A = 0.5$ (curve d).The general dependence of T_C with D is quite similar to the case of the system with $S_A = \frac{1}{2}$ and $S_B = 1$. The large negative values of D remain the sublattice spins S_B^z in the lower states $\pm\frac{1}{2}$, while the enough positive values are favorable to keep the spins S_B^z in their higher states $\pm\frac{3}{2}$. Note that for a given value of (D, J_B/J_A), T_C increases almost linearly with J_{AB}/J_A.The compensation temperature as a function of D/J_A is also depicted in the same figure 3. One can notice that for a given value of J_{AB}/J_A, T_{comp} depends strongly on D over a narrow and asymmetric interval (for example, $-0.26 \leq D/J_A \leq +0.58$ for $J_{AB}/J_A = 0.05$). In the outside of this interval, the compensation temperature becomes almost constant and in particular for negative D,T_{comp} draws practically to zero. Also, for small inter-sublattice coupling ($J_{AB}/J_A \lesssim 0.05$) and large positive values of D ($D/J_A \gtrsim 2$), we note that T_{comp} becomes almost independent of D. The existence of T_{comp} for given values of D and J_B is related to the J_{AB}/J_A ratio. For example, when $D = 0$ and $J_B/J_A = 0.01$, the compensation temperature disappears at $J_{AB}/J_A = 0.35$.

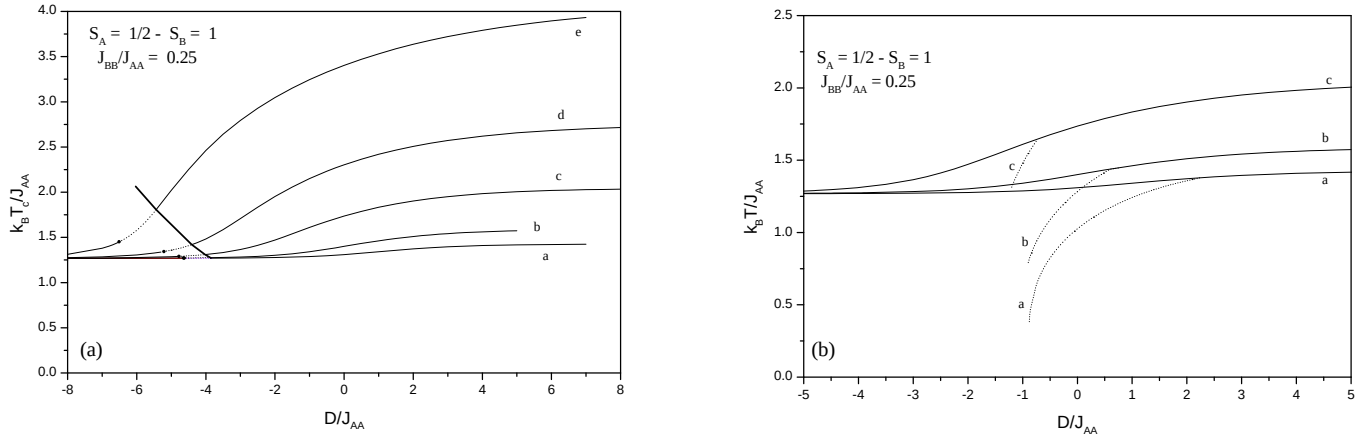

FIG. 2: (a) Phase diagram of the two-sublattice system with $S_A = \frac{1}{2}$ and $S_B = 1$ in the (D, T) plane. The value of J_B/J_A is then fixed at $J_B/J_A = 0.25$ and the value of J_{AB}/J_A is changed from $J_{AB}/J_A = 0.05$ (curve a) to 1.0 (curve e). The solid and dashed curves represent respectively the second and the first order transition. The thick line indicates the tricritical points. (b) Phase diagram for $J_B/J_A = 0.25$ and different values of J_{AB}/J_A : 0.01 (curve a), 0.1 (curve b), 0.25 (curve c). The solid and dashed curves represent respectively T_C and the compensation temperature T_{comp} .

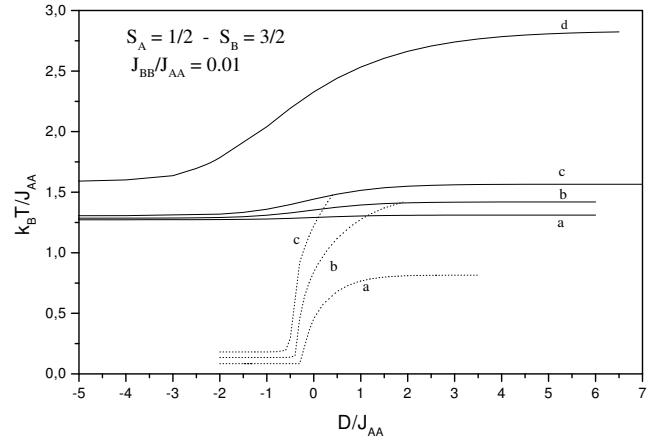

FIG. 3: Phase diagram of the two-sublattice system with $S_A = \frac{1}{2}$ and $S_B = \frac{3}{2}$ when the value of D/J_A is changed. The value of J_B/J_A is fixed at 0.01 and the value of J_{AB}/J_A is changed, $J_{AB}/J_A = 0.05$ (curve a), $J_{AB}/J_A = 0.1$ (curve b), $J_{AB}/J_A = 0.15$ (curve c) and $J_{AB}/J_A = 0.5$ (curve d). The solid and dashed curves mean respectively T_C and T_{comp} .

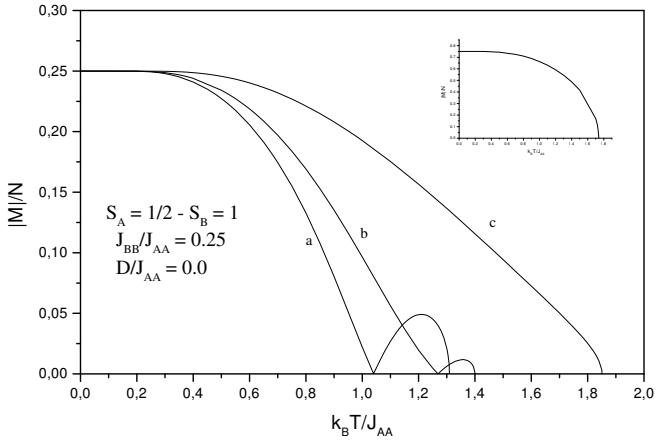

FIG. 4: The thermal variations of the total magnetization per site $\frac{|M|}{N}$ in two-sublattice system with $S_A = \frac{1}{2}$ and $S_B = 1$. $D = 0.0$ with $J_B/J_A = 0.25$ and changing J_{AB}/J_A: $J_{AB}/J_A = 0.05$ (curve a), $J_{AB}/J_A = 0.1$ (curve b) and $J_{AB}/J_A = 0.5$ (curve c). In the insert, the comparison with the uncoupled ferromagnetic layers ($J_{AB}/J_A = 0$) is shown.

C. Magnetization curves

In this section, we investigate the temperature dependences of magnetization in the two-sublattices system by solving numerically the coupled equations (28)-(30) for selected values of D/J_A, J_{AB}/J_A and J_B/J_A.

Note that the total magnetization per site $\frac{M}{N}$ is defined as:

$$\frac{M}{N} = \frac{1}{2}(m_A + m_B)$$

1. *Two-sublattice system with $S_A = \frac{1}{2}$ and $S_B = 1$*

In Fig. 4, the thermal variations of $\frac{M}{N}$ are plotted for $D = 0.0$ with $J_B/J_A = 0.25$ and changing J_{AB}/J_A from $J_{AB}/J_A = 0$ (curve a) to $J_{AB}/J_A = 0.5$ (curve d). As depicted in Fig. 4, the magnetization curves exhibit some outstanding features. In particular, for lower values of interplanar coupling ($J_{AB}/J_A \leq 0.14$) there exists a compensation temperature which decreases with J_{AB}/J_A. For larger values of J_{AB}/J_A ($J_{AB}/J_A > 0.14$), the magnetization curves are typically of Q-type in the Néel classification nomenclature [1].

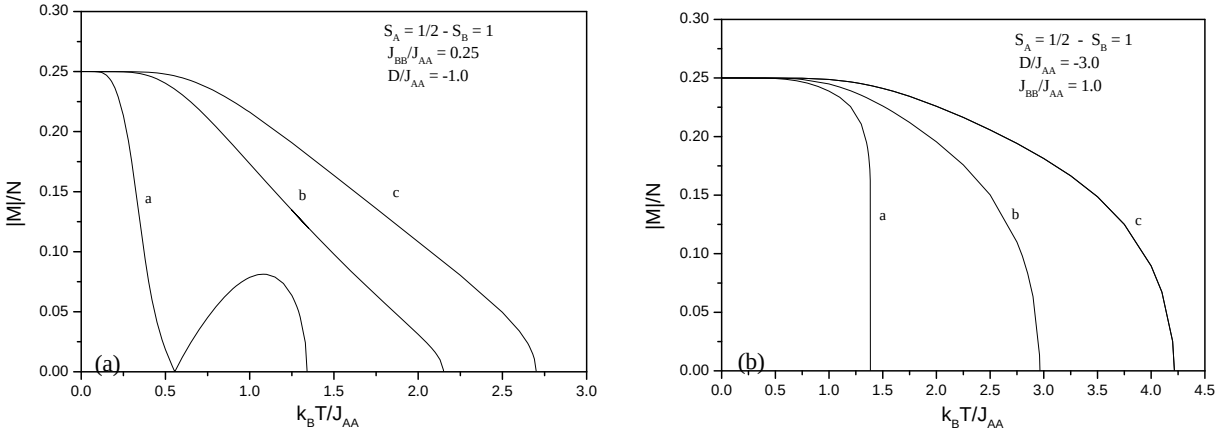

FIG. 5: (a) The total magnetization per site $\frac{|M|}{N}$ as a function of temperature in two-sublattice system with $S_A = \frac{1}{2}$ and $S_B = 1$ for $D/J_A = -1$ with $J_B/J_A = 0.25$ and changing J_{AB}/J_A from $J_{AB}/J_A = 0.1$ (curve a), $J_{AB}/J_A = 0.5$ (curve b) and $J_{AB}/J_A = 0.75$ (curve c).
(b) The total magnetization per site $\frac{|M|}{N}$ as a function of temperature in two-sublattice system with $S_A = \frac{1}{2}$ and $S_B = 1$ for $D/J_A = -3$ with $J_B/J_A = 1$ and changing J_{AB}/J_A from $J_{AB}/J_A = 0.05$ (curve a), $J_{AB}/J_A = 0.5$ (curve b) and $J_{AB}/J_A = 1$ (curve c). Note that the curve a shows a first transition order.

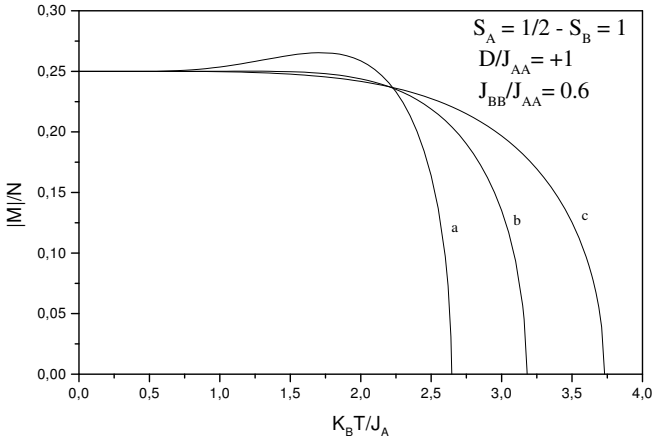

FIG. 6: The thermal variations of $\frac{|M|}{N}$ in two-sublattice system with $S_A = \frac{1}{2}$ and $S_B = 1$ for positive value of the anisotropy constant ; $D/J_A = +1$, with $J_B/J_A = 0.6$ and changing J_{AB}/J_A: $J_{AB}/J_A = 0.25$ (curve a), $J_{AB}/J_A = 0.5$ (curve b) and $J_{AB}/J_A = 0.75$ (curve c).

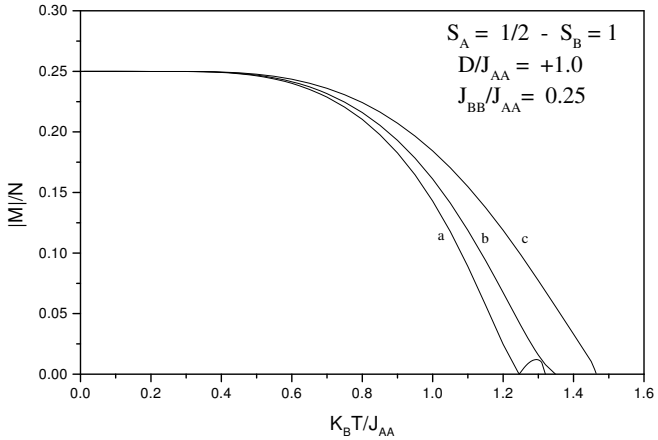

FIG. 7: The thermal variations of $\frac{|M|}{N}$ in two-sublattice system with $S_A = \frac{1}{2}$ and $S_B = 1$ for $D/J_A = +1$, with $J_B/J_A = 0.25$ and variuous values of J_{AB}/J_A: $J_{AB}/J_A = 0.04$ (curve a), $J_{AB}/J_A = 0.06$ (curve b) and $J_{AB}/J_A = 0.1$ (curve c).

In Fig. 5, the thermal variations of $\frac{M}{N}$ are plotted for $D = -1$ with $J_B/J_A = 0.25$ and changing J_{AB}/J_A from $J_{AB}/J_A = 0$ (curve a) to $J_{AB}/J_A = 1.0$ (curve e). The compensation point is present only for $J_{AB}/_A \leq 0.3$.

In Fig. 6, the thermal variations of $\frac{M}{N}$ are plotted for positive value of the anisotropy constant ; $D = +1$, with $J_B/J_A = 0.6$ and changing J_{AB}/J_A from $J_{AB}/J_A = 0$ (curve a) to $J_{AB}/J_A = 1.0$ (curve e). The magnetization curves don't express any compensation point, but they manifest certain special behaviors. In particular, M changes from the P-type behavior of the curve a to the usual Q-type behavior (after the Néel Classification) when the value of J_{AB}/J_A increases up to 0.5. But, the N-type behavior exhibiting the compensation point is not found in Fig. 6.

However, the N-type behavior is also possible when the value of $J_B/J_A$is lowered. For example, when we get $J_B/J_A = 0.25$, we obtain a compensation temperature $1.13 \leq \frac{k_B T_{comp}}{J_A} \leq 1.55$ by changing J_{AB}/J_A respectively from 0 to 0.042 as depicted in Fig.7. Thus, we can conclude that the increase of J_B/J_A has the effect of keeping the system ordered at higher temperatures such that the critical point T_C occurs at higher temperatures. Here, we are limited to the ferrimagnetic cases ($J_{AB}/J_A \geq 0$), the ferromagnetic study will be presented elsewhere[29].The

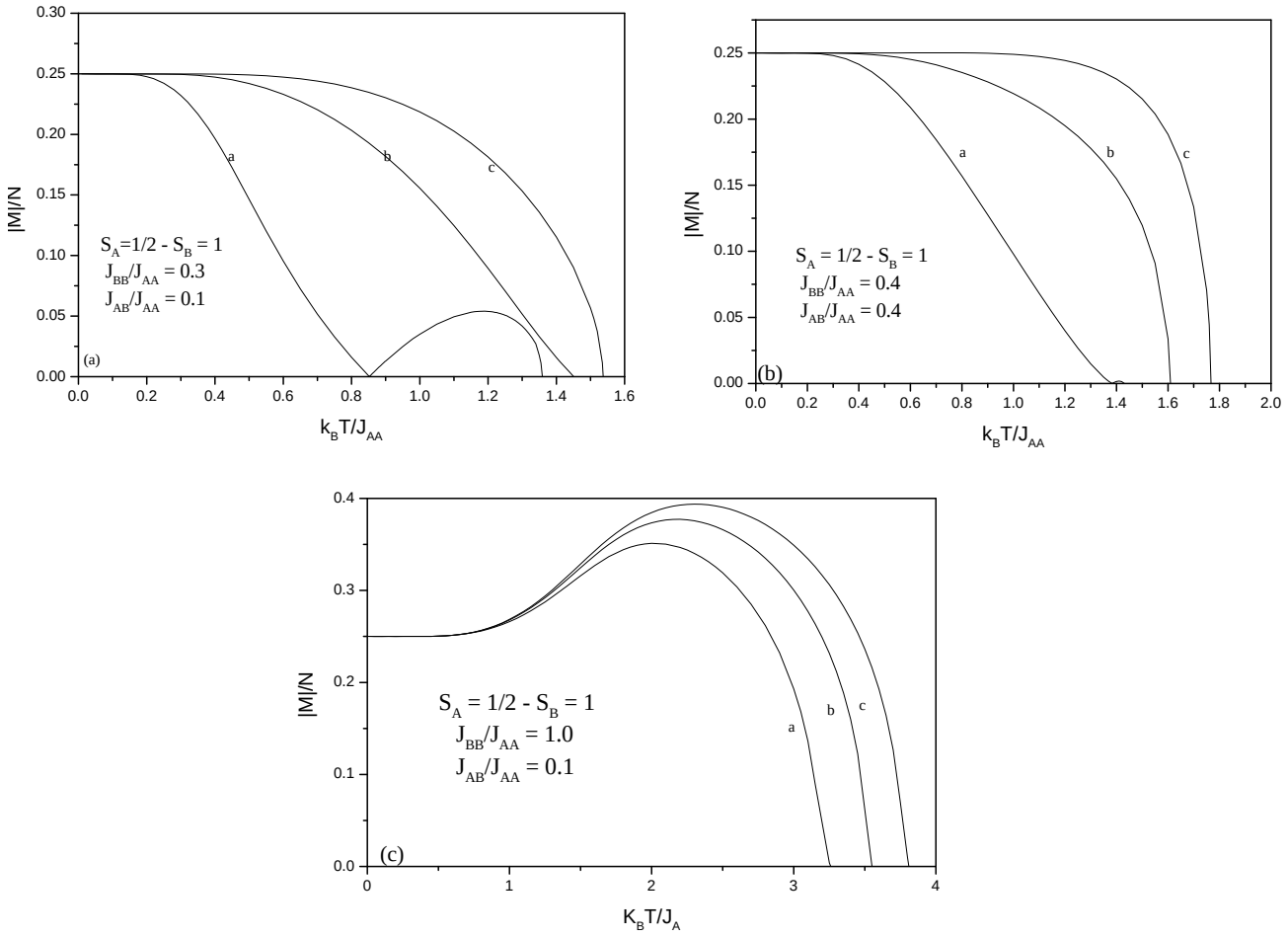

FIG. 8: Illustration of the D influence in two-sublattice system with $S_A = \frac{1}{2}$ and $S_B = 1$ for $J_{AB}/J_A = 0.1$ and selected sets of J_B/J_A: 0.30 (Fig.8 a), 0.40 (Fig.8 b) and 1.0.(Fig.8 c). Notice that the system goes from the N-type to the Q-type behaviors when D/J_A changes from -1 (curves a) to 0 (curves b) or $+1$(curves c).

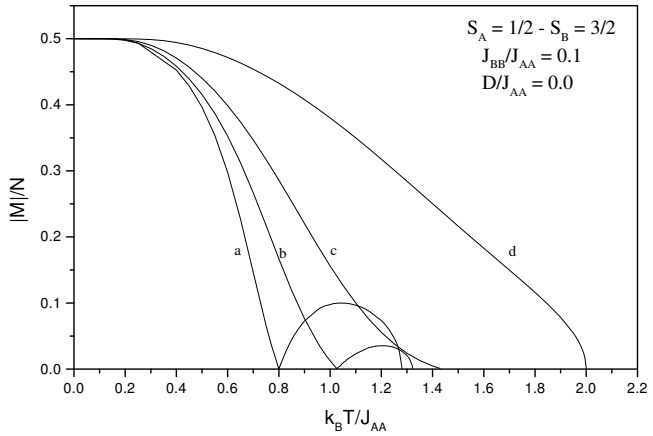

FIG. 9: The thermal variations of $\frac{|M|}{N}$ in the two-sublattice system with $S_A = \frac{1}{2}$ and $S_B = \frac{3}{2}$ for $D/J_A. = 0$ and $J_B/J_A = 0.1$ when J_{AB}/J_A is changing from $J_{AB}/J_A = 0.02$ (curve a) to $J_{AB}/J_A = 0.5$ (curve d).

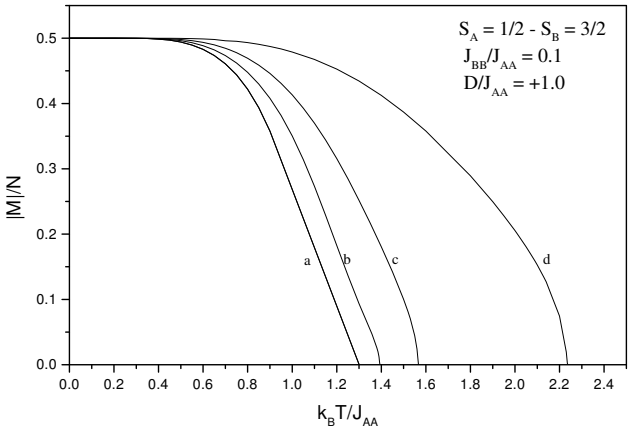

FIG. 10: The thermal variations of $\frac{|M|}{N}$ in the two-sublattice system with $S_A = \frac{1}{2}$ and $S_B = \frac{3}{2}$ for $D/J_A. = +1$ and $J_B/J_A = 0.1$ when J_{AB}/J_A is changing from $J_{AB}/J_A = 0.02$ (curve a) to $J_{AB}/J_A = 0.3$ (curve d).

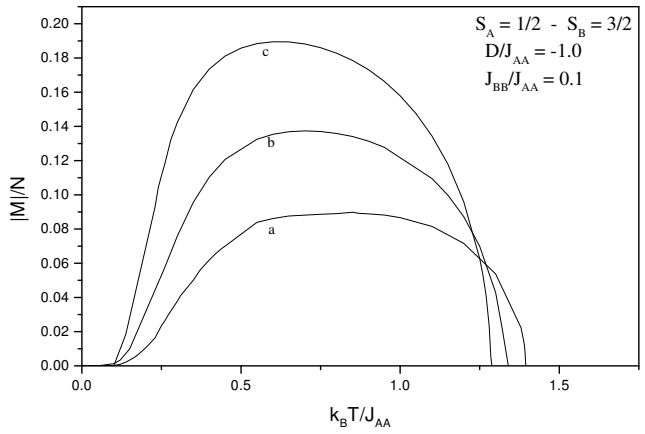

FIG. 11: The thermal variations of $\frac{|M|}{N}$ in the two-sublattice system with $S_A = \frac{1}{2}$ and $S_B = \frac{3}{2}$ for $D/J_A. = -1$ and $J_B/J_A = 0.1$ when J_{AB}/J_A is changing from $J_{AB}/J_A = 0.15$ (curve a) to $J_{AB}/J_A = 0.10$ (curve b) or $J_{AB}/J_A = 0.15$.

influence of D is clearly illustrated in theFigs.8a, b and c for the selected values $J_B/J_A = 0.3$ and $J_{AB}/J_A = 0.10$. We notice that the system goes from the N-type to the Q-type behaviors when D/J_A changes from -1 to 0 or $+1$.

2. *Two-sublattice system with $S_A = \frac{1}{2}$ and $S_B = \frac{3}{2}$*

In Fig. 9, 10 and 11, the various kinds of $\frac{|M|}{N}$ curves that can occur are shown for selected values of J_B/J_A, J_{AB}/J_A and D/J_A.In particular, for negative D ($D = -1$) and small values of J_{AB}/J_A, M exhibits a L-type in the Néel theory as depicted in the curves ($J_B/J_A = 0.1$, $J_{AB}/J_A = 0.05$) and ($J_B/J_A = 0.1$,$J_{AB}/J_A = 0.1$) where the saturation value at $T = 0K$ is zero, due to the $S^z_{mB} = \pm\frac{1}{2}$ state in the sublattice B. According to Fig. 9, 10 and 11, the existence of compensation temperature is affected by the inter-sublattice coupling J_{AB}/J_A besides the different crystal-field constants $D/J_A = 0, 1$ or -1. These results may be compared to those obtained in the square lattice case with $z = 4$ by Kaneyeoshi et al.[28] and those consisting in Monte Carlo simulation that are achieved very recently by Buendia et al. [30].

VI. CONCLUSION

In this work, we have investigated the phase diagrams and magnetization behaviors of a two-sublattice ferrimagnetic system with spins $S_A = \frac{1}{2}$ and $S_B = 1$ or $S_B = \frac{3}{2}$ on a triangular lattice, by the use of the effective-field theory. Furthermore the high coordinate number $z = 6$, the spins are coupled by tree exchange interactions and the crystal field acting on the spins S_B. We have showed through the above discussion that each exchange coupling affects all magnetic properties of every sublattice in the system. Moreover, we have illustrated the peculiar role of the single ion anisotropy in the apparition of the compensation temperature. We think that the results obtained here may be useful for the comprehension of magnetic properties of some special materials such the lamellar oxides [15]; [16]; [17], the GBIC's [22], and similar layered compounds in which the magnetic entities have a high coordinate number ($z = 6$).The effects of applied magnetic fields and the susceptibility behaviors will be investigated in a nearby study [29].

VII. APPENDIX A

The expressions of the parameters $\overline{a}$ *and* $\overline{b}$ in Eq. (36) are given by:

$$1 - \overline{a} = [1 - V_1][1 - U_1] - V_2U_2$$

and

$$\overline{b} = 3U_3 - 3U_3V_1 + V_3(1 - U_1) - (2U_3U_2V_2)/(1 - U_1) + U_2V_4 + (U_2^2V_5)/(1 - U_1) + \frac{(U_2^3V_6)}{(1 - U_1)^2}$$

where

$$U_1 = 12L_{21}\ ; U_2 = -6L_{12};\ U_3 = 180L_{23}\ ;$$
$$V_1 = 6T_{12}\ ;\ V_2 = -12T_{21}\ ;\ V_3 = 20T_{14};$$
$$V_4 = -180T_{23}\ ;\ V_5 = 360T_{32}\ ;\ V_6 = -160T_{41}$$

[1] L. Néel, Ann. Phys. (Paris) 3 (1948)37
[2] B. Barbara, D. Gignoux and C. Vettier, *Lectures on Modern Magnetism*, (Science Press, Beijing, Springer-Verlag, Berlin (1988)
[3] T. Kaneyoshi and J.C. Chen, J.M.M.M 98(1991)201
[4] T. Kaneyoshi J. Phys. Soc. Jpn. 56(1987)22675
[5] A. Benyoussef, A. El Kenz and T. Kaneyoshi, J.M.M.M 131(1994) 173 and 131(1994) 179
[6] T. Iwashita and N. Uryu, J. Phys. Soc. Jpn. 53 (1984)721
[7] F. Verona De Resende, F.C. Sa Barreto and J.A. Plascak, Physica 149A(1988)606
[8] N. Benayad and J. Zittartz, Z. Phys. B 81 (1990) 107
[9] B.Y. Yousif and R.G Bowers, J. Phys. A17, (1984) 3389
[10] G.M. Zhang and Ch.Z. Yang, Phys. Rev. B48 (1993) 9452
[11] J.W Tucker, J. Mag. Mag. Mat. 195(1999)733
[12] M. Fresneau, A. Vilouvet and A. Khater, J. Mag. Mag. Mat. 202(1999)220
[13] R. Honmura and T. Kaneyoshi, J. Phys. C 12 (1979) 3979

[14] T. Kaneyoshi, Acta Polon. A 83(1993) 703
[15] K.Hirota, Y.Nakazawa and M.Ishikawa, J.Phys.Condens. Matter 4 (1992)6291
[16] G.Dutta, A.Manthiram, J.B.Goodenough and J.C.Grenier, J.Solid St. Chem.96(1992)123
[17] R.Stoyanova, E.Hecheva and C.Friebel, Solid St. Ionics 73 (1994)1
[18] A. Bajpai, A. Banerjee, Phys. Rev. B 55 (1997)12439
[19] A. Hérold, G. Furdin, G. Guérard, L. Hachim, N.E. Nadi and R. Vangelisti, Ann. Phys. (Paris) Colloq. 11, C2-3 (1986)
[20] M. Suzuki, I. Oguro and Y. Jinzaki, J. Phys. C 17, (1984)L575
[21] S. Chehab, P. Biensan, S. Flandrois and J. Amiell, Phys. Rev. B 45 No 6 (1992) 2844
[22] M. El Hafidi, J.M. Louis, G. Chouteau,P. Biensan and C. Delmas, Solid State Comm. 101(1997)699 and references therein
[23] T. Kaneyoshi in *New Trends in Magnetism, Magnetic Materials and their applications*, ed. J.M. Lopez and J.M. Sanchez, Plenum Press, U.S.A 1996
[24] H. B Callen, Phys. Lett. 4(1963)161
[25] M. Suzuki, Phys. Lett. 19 (1965)267
[26] T. Kaneyoshi, J.W. Tucker and M. Jascur, Physica A 186 (1992) 495
[27] I. Syozi and H. Nakano, Prog. Theoret. Phys. 13(1955)69
[28] T. Kaneyoshi and M. Jascur, Physica A 195(1993) 474
[29] M. Aouzi and M. El Hafidi, to be published
[30] G.M. Buendia and R. Cardona, Phys. Rev. B 59 (10) (1999)6784